

Embedded NDE with Piezoelectric Wafer Active Sensors in Aerospace Applications

Victor Giurgiutiu

The capability of embedded piezoelectric wafer active sensors (PWAS) to perform in-situ nondestructive evaluation (NDE) is explored. Laboratory tests are used to prove that PWAS can satisfactorily perform Lamb wave transmission and reception. Subsequently, crack detection in an aircraft panel with the pulse-echo method is illustrated. For large area scanning, a PWAS phased array is used to create the embedded ultrasonics structural radar (EUSR). For quality assurance, PWAS are self-tested with the electromechanical impedance method.

INTRODUCTION

Embedded nondestructive evaluation (NDE) is an emerging technology that will allow transitioning the methods of conventional ultrasonics to embedded systems structural health monitoring (SHM) such as those envisioned for the Integrated Vehicle Health Management (IVHM). SHM for IVHM- requires the development of small, lightweight, inexpensive, unobtrusive, minimally invasive sensors to be embedded in the airframe with minimum weight penalty and at affordable costs [1]. Such sensors should be able to scan the structure and identify the presence of defects and incipient damage.

Current ultrasonic inspection of thin wall structures (e.g., aircraft shells, storage tanks, large pipes, etc.) is a time consuming operation that requires meticulous through-the-thickness C-scans over large areas. One method to increase the efficiency of thin-wall structures inspection is to utilize guided waves (e.g., Lamb waves) instead of the conventional pressure waves [2,3,4]. Guided waves propagate along the mid-surface of thin-wall plates and shallow shells. They can travel at relatively large distances with very little amplitude loss and offer the advantage of large-area

coverage with a minimum of installed sensors [5,6]. Guided Lamb waves have opened new opportunities for cost-effective detection of damage in aircraft structures [7], and a large number of papers have recently been published on this subject [8]. Traditionally, guided waves have been generated by impinging

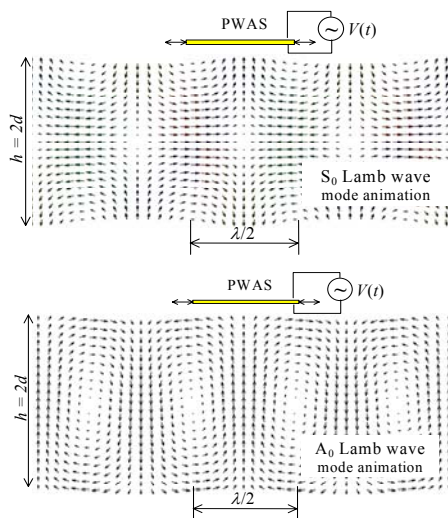
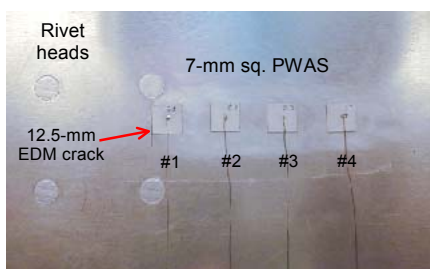


Figure 1 – Piezoelectric wafer active sensors (PWAS) mounted on aircraft panel (b) PWAS interaction with Lamb modes (click on figure for animation)

the plate obliquely with a tone-burst from a relatively large ultrasonic transducer [9]. Snell's law ensures mode conversion at the interface, hence a combination of pressure and shear waves are simultaneously generated into the thin plate. However, conventional Lamb-wave probes (wedge and comb

transducers) are relatively too heavy and expensive to be considered for widespread deployment on an aircraft structure as part of a SHM system. Hence, a different type of sensors than the conventional ultrasonic transducers is required for the SHM systems.

Several investigators [10-12] have recently explored the generation of Lamb-waves with piezoelectric wafer active sensors (PWAS)[13]. PWAS are inexpensive, non-intrusive, un-obtrusive, and minimally invasive devices that can be surface-mounted on existing structures inserted between the layers of lap joints, or inside composite materials. Figure 1a shows an array of 7 mm square PWAS mounted on an aircraft panel, adjacent to rivet heads and an electric discharge machined (EDM) simulated crack. The minimally invasive nature of the PWAS devices is apparent. These PWAS weight around 68 mg, are 0.2 mm thick, and cost \$7. PWAS operated on the piezoelectric principle that couples the electrical and mechanical variables in the material (mechanical strain, S_{ij} , mechanical stress, T_{kl} , electrical field, E_k , and electrical displacement D_j) in the form:

$$\begin{aligned} S_{ij} &= s_{ijkl}^E T_{kl} + d_{kij} E_k \\ D_j &= d_{jkl} T_{kl} + \epsilon_{jk}^T E_k \end{aligned} \quad (1)$$

where s_{ijkl}^E is the mechanical compliance of the material measured at zero electric field ($E = 0$), ϵ_{jk}^T is the dielectric permittivity measured at zero mechanical stress ($T = 0$), and d_{kij} represents the piezoelectric coupling effect. For embedded NDE applications, PWAS couple their in-plane motion, excited by the applied oscillatory voltage through the piezoelectric effect, with the Lamb-waves particle motion on the material surface. Lamb waves can be either quasi-axial (S_0, S_1, S_2, \dots), or

quasi-flexural (A0, S1, S2, ...) as shown in Figure 1b,c. PWAS probes can act as both exciters and sensor of the elastic Lamb waves traveling in the material.

For NDE, PWAS can be used as both active and passive probes. Thus, they address four IVHM-SHM needs [14-16]:

- 1) Far-field damage detection using pulse-echo and pitch-catch methods
- 2) Near-field damage detection using

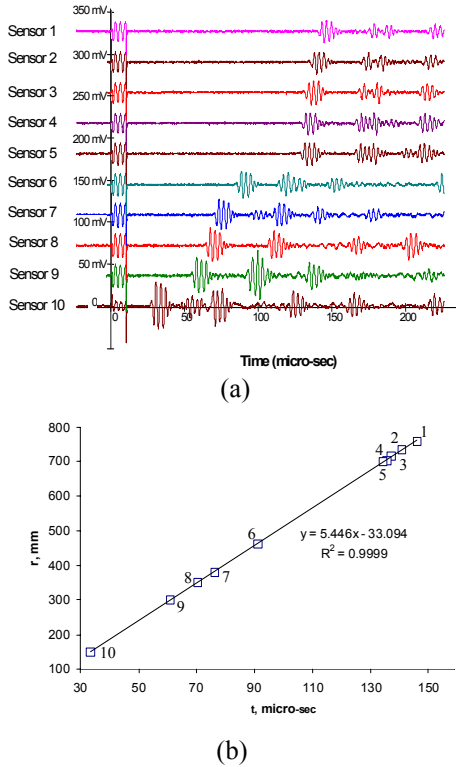


Figure 2 (a) Reception signals on active sensors 1 through 10; (b) correlation between radial distance and time of flight.

- 3) Acoustic emission monitoring of crack initiation and growth
 - 4) Low-velocity impact detection
- PWAS operation is different than that of conventional ultrasonic probes:

(a) PWAS achieve Lamb wave excitation and sensing through surface “pinching” (in-plane strains), while conventional ultrasonic probes excite through surface “tapping” (normal stress).

(b) PWAS are strongly coupled with the structure and follow the structural dynamics, while conventional ultrasonic probes are relatively free from the structure and follow their own dynamics.

(c) PWAS are non-resonant wide-band devices, while conventional

ultrasonic probes are narrow-band resonators.

The main advantage of PWAS over conventional ultrasonic probes lies in their small size, lightweight, low profile, and small cost. In spite of their small size, these novel devices are able to replicate many of the functions that the conventional ultrasonic probes, as proven by the proof-of-concept laboratory demonstrations described next.

PWAS GENERATED LAMB WAVES

The basic principles of Lamb wave generation and detection by PWAS probes were first verified on simple laboratory experiments. A 1.6-mm thick, 2024-aluminum alloy rectangular plate (914mm x 504mm x 1.6 mm) was instrumented with eleven 7-mm sq., 0.2-mm thick PWAS (American Piezo Ceramics Inc., APC-850) placed on a rectangular grid. We this setup, we verified that: (a) Lamb waves can be satisfactorily generated and detected with PWAS; (b) omnidirectional transmission is achieved; and (c) signals are strong enough and attenuation is sufficiently low for echoes to be detected. The proof of these attributes is especially important for PWAS, which are at least an order of magnitude smaller and lighter than conventional ultrasonic transducers, and hence utilize much lower power.

To prove that the Lamb waves excited by PWAS are omnidirectional, we used one PWAS (#11) as transmitter and the other PWAS (#1–10) as receivers. The signals observed in this investigation are shown in Figure 2a. In each row, the electromagnetic coupling of the ‘initial bang’ is shown around the origin. Then, the first wave package corresponding to the wave received from the transmitter PWAS is seen, followed by other wave packages corresponding to reflections from the plate edges. The time difference between the initial bang and the wave-package arrival represents the time-of-flight (TOF). The TOF is consistent with the distance traveled by the wave. Figure 2b shows the straight-line correlation between TOF and distance. The slope of this line is the experimental group velocity, $c_g = 5.446$ km/s. The theoretical value should be 5.440 km/s. Very good accuracy is

observed (99.99% correlation; 0.1% speed detection error). Thus, we proved (a) and (b), i.e., that PWAS-generated Lamb waves propagate are “loud and clear”, propagate omnidirectionally, and correlate well with the theory.

PULSE-ECHO WITH PWAS

PWAS #11 was used for the demonstration of pulse-echo capabilities. Figure 3a, which shows that the sensor #11 signal has two distinct zones: (i) the

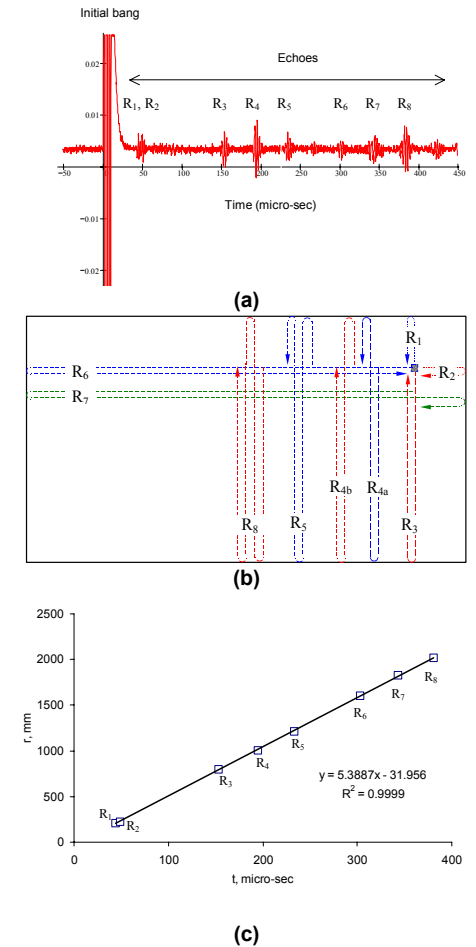


Figure 3 – Pulse-echo method applied to active sensor #11: (a) the excitation signal and the echo signals on active sensor #11; (b) schematic of the wave paths for each wave pack; (c) initial bang, during which the PWAS #11 acts as transmitter; and (ii) the echoes zone, containing wave packs reflected by the plate boundaries and sent back to PWAS #11. These echoes were processed to evaluate the pulse-echo capabilities of the method. Since the wave generated by the initial bang underwent multiple reflections from the plate edges, each of these reflections had a different path length, as shown in

Figure 3b. It is interesting to note that the path lengths for reflections R_1 and R_2 are approximately equal. Hence, the echoes R_1 and R_2 in the pulse-echo signal of Figure 3a are almost superposed.

Also interesting to note is that the reflection R_4 has two possible paths, R_{4a} and R_{4b} of same length. Hence, the echoes corresponding to these two reflection paths arrive simultaneously and form a single but stronger echo signal, which has roughly twice the intensity of the other echoes. A plot of the TOF of each echo vs. its path length is given in Figure 3c. The straight line fit has a very good correlation ($R^2 = 99.99\%$). The corresponding wave speed is 5.389 km/s, i.e., within 1% of the theoretical value of 5.440 km/s. The echoes were recorded from over 2,000 mm distance, which is remarkable for such small ultrasonic devices. Thus, it was proved that the PWAS are fully capable of transmitting and receiving pulse-echo signals of remarkable strength and clarity.

PWAS CRACK DETECTION

Wave propagation experiments were conducted on an aircraft panel to illustrate crack detection through the pulse-echo method. The panel has a typical aircraft construction, featuring a vertical splice joint and horizontal stiffeners. Figure 4 shows three photographs of PWAS installation on increasingly more complex structural regions of the panel. Adjacent to the photographs are the PWAS signals. All the experiments used only one PWAS, operated in pulse-echo mode. The PWAS was placed in the same relative location, i.e., at 200 mm to the right of the vertical splice joint. The first row of Figure 4 shows the situation with the lowest complexity, in which only the vertical splice joint is present in the far left. The signal to the right of this photograph shows the initial bang (centered at around 5.3 micro-sec) and multiple reflections from the panel edges and the splice joint. The echoes start to arrive at approximately 60 μ s. The second row of Figure 4 shows the vertical row of rivets in the far left and, in addition, a horizontal double row of rivets stretching towards the PWAS. The signal to the right shows that, in addition to the

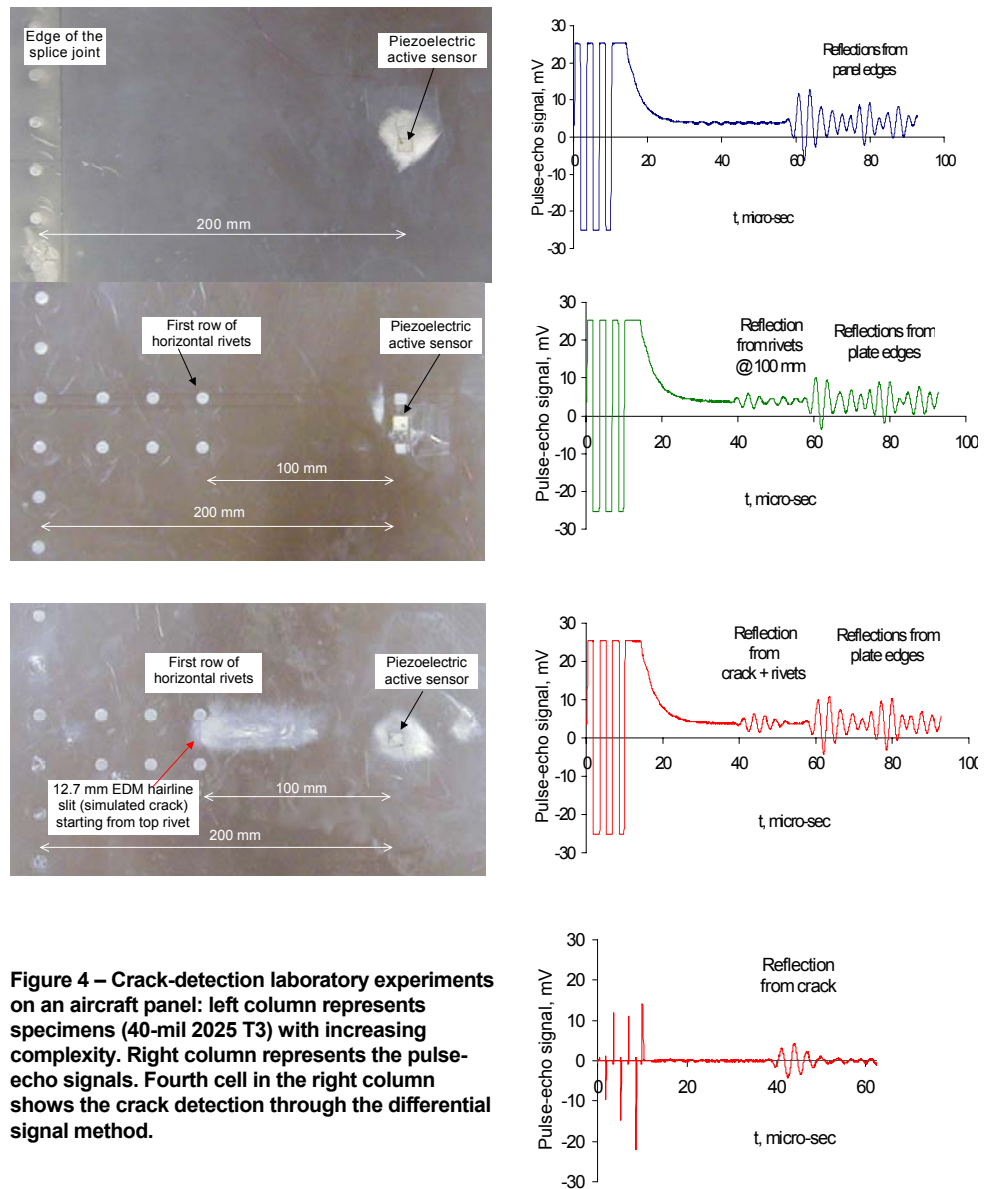


Figure 4 – Crack-detection laboratory experiments on an aircraft panel: left column represents specimens (40-mil 2025 T3) with increasing complexity. Right column represents the pulse-echo signals. Fourth cell in the right column shows the crack detection through the differential signal method.

multiple echoes from the panel edges and the splice, the PWAS also receives backscatter echoes from the rivets located at the beginning of the horizontal row. These backscatter echoes are visible at around 42 μ s. The third row in Figure 4 shows a region of the panel similar to that presented in the previous row, but having an addition feature: a simulated crack (12.7-mm EDM hairline slit) emanating from the first rivet hole in the top horizontal row. The signal at the right of this photo shows features similar to those of the previous signal, but somehow stronger at the 42 μ s. The features at 42 μ s correspond to the superposed reflections from the rivets and from the crack. The detection of the crack seems particularly difficult because

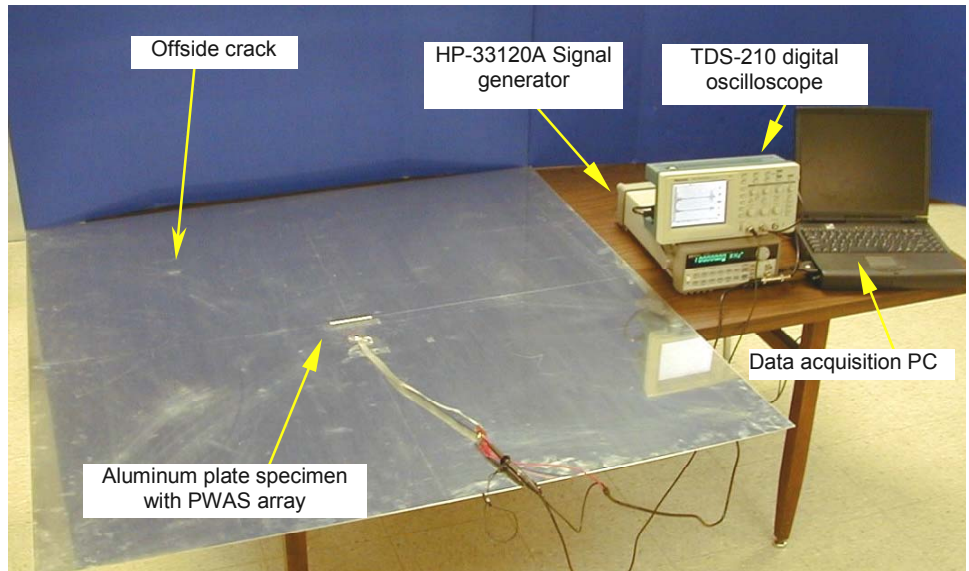
the echoes from the crack and from the rivets are superposed.

This difficulty was resolved by using the differential signal method, i.e., subtracting the signal presented in the second row from the signal presented in the third row. In practice, such a situation would correspond to subtracting a signal previously recorded on the undamaged structure from the signal recorded now on the damaged structure. Such a situation of using archived signals is typical of health monitoring systems. When the two signals were subtracted, the result presented in the last row of Figure 4 was obtained. This differential signal shows a “loud and clear” echo due entirely to the crack. The echo, marked “reflection from the crack” is centered at 42 μ s, i.e., TOF

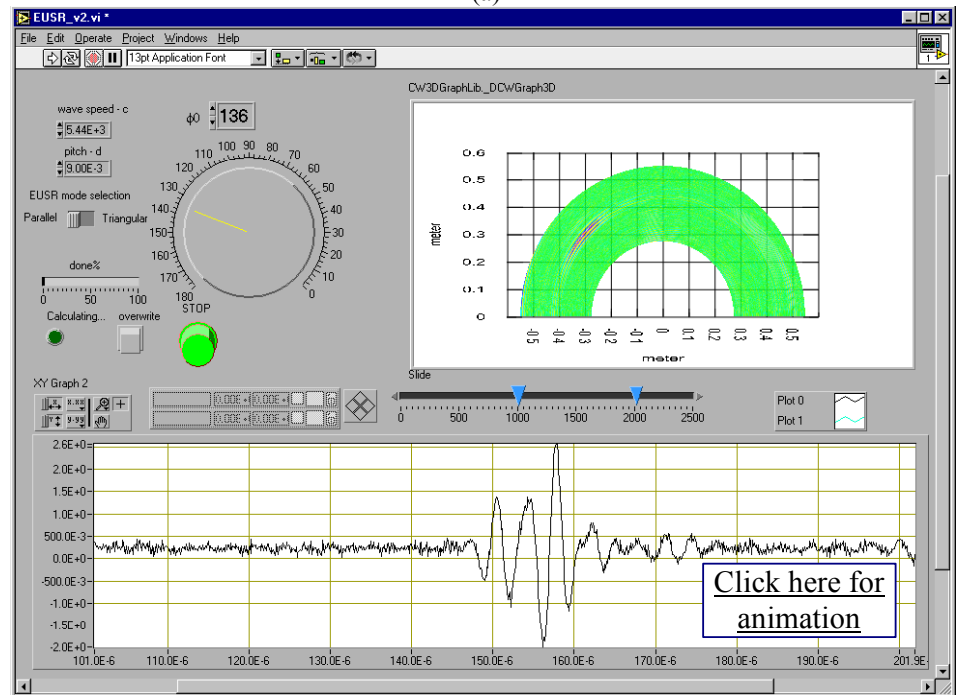
= 37 μ s which correlates very well with a 5.4 km/s 200-mm total travel from the PWAS to the crack placed at 100 mm. The cleanness of the crack-detection feature and the quietness of the signal ahead of the crack-detection feature are remarkable. Thus, we concluded that PWAS are capable of clean and unambiguous detection of structural cracks.

PWAS PHASED ARRAYS

The advantages of phased array transducers for ultrasonic testing are multiple [17,18]. Krautkramer, Inc. [19] produces a line of phased array transducers for the inspection of very thick specimens, and in the sidewise inspection of thick slabs, etc. These transducers employ pressure waves generated through normal impingement on the material surface. In our research [20], we have developed a phased array technology for thin wall structures (e.g., aircraft shells, storage tanks, large pipes, etc.) that uses Lamb waves to cover a large surface area through beam steering from a central location. We called this concept *embedded ultrasonics structural radar* (EUSR) and constructed a simple proof-of-concept experiment (Figure 5a). A PWAS array was made up of a number of identical 7-mm sq. elements aligned at uniform 9-mm pitch. The PWAS phased array was placed at the center of a 4-ft square thin aluminum plate (Figure 5a). The wave pattern generated by the phased array is the result of the superposition of the waves generated by each individual element. By sequentially firing the individual elements of an array transducer at slightly different times, the ultrasonic wave front can be focused or steered in a specific direction. Thus, we achieved electronic sweeping and/or refocusing of the beam without physical manipulating the transducers. We proved that inspection of a wide zone is possible by creating a sweeping beam of ultrasonic Lamb waves that covered the whole plate. Once the beam steering and focusing was established, the detection of crack was done with the pulse-echo method. During these proof-of-concept experiments, the EUSR methodology was used to detect cracks in two typical situations: (i) a 19-mm broadside crack placed at 305 mm from the array in the 90 deg direction; and (ii) a 19-mm



(a)



(b)

Figure 5 – Proof-of-concept EUSR experiment: (a) thin plate specimen 9-element PWAS array and 19-mm offside crack; (b) Graphical user interface (EUSR-GUI) front panel. The angle sweep is performed automatically to produce the structure/defect imaging picture on the right. Manual sweep of the beam angle can be also performed with the turn knob; the signal reconstructed at the particular beam angle (here, $\phi = 136$ deg) is shown in the lower picture.

broadside crack placed at 409 mm from the array in the 136 deg direction. Of these two, the latter was more challenging because the ultrasonic beam is not reflected back to the source but rather deflected sideways. Hence, the echo received from the offside crack is merely the backscatter signal generated at the crack tips. Figure 5b presents the front panel of the embedded ultrasonic

structural radar graphical user interface (EUSR-GUI) displaying the offside signals. The sweep is performed automatically to produce the structural defect image in the right pane. Manual sweep can be performed with the turn knob. The reconstructed signal is shown in the lower pane. In Figure 5b, the lower pane show the signal reconstructed at the beam angle $\phi_0 = 136$ deg corresponding

structural radar graphical user interface (EUSR-GUI) displaying the offside signals. The sweep is performed automatically to produce the structural defect image in the right pane. Manual sweep can be performed with the turn knob. The reconstructed signal is shown in the lower pane. In Figure 5b, the lower pane show the signal reconstructed at the beam angle $\phi_0 = 136$ deg corresponding

to the crack location. An animation of the crack detection methodology can be visualized using [click here](#) in Figure 5b.

PWAS SELF-TEST

Since the PWAS probes are adhesively bonded to the structure, the bond durability and the possibility of the probe becoming detached are of concern. To address this, we have identified a PWAS self-test procedure that can reliably determine if the sensor is still perfectly attached to the structure, or not. The procedure is based PWAS in-situ electromechanical impedance [14, 15].

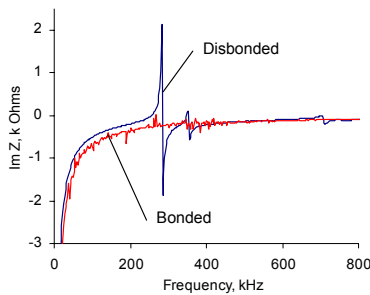


Figure 6 – PWAS self test: when sensor is disbonded, a clear free-vibration resonance appears at ~267 kHz

Figure 6 compares the Im Z spectrum of a well-bonded PWAS with that of a disbonded (free) PWAS. The well-bonded PWAS presents a smooth Im Z curve, modulated by small structural resonances. The disbonded PWAS shows a strong self-resonance, and no structural resonances. The appearance of the PWAS resonance and the disappearance of structural resonances constitute features that can unambiguously discern when the PWAS has become disbonded, and can be used for automated PWAS self-test. For a partially disbonded PWAS, a mixture of PWAS and structure vibration was recorded.

CONCLUSION

This paper has presented a novel structural health-monitoring concept – embedded NDE piezoelectric wafer active sensors (PWAS). PWAS can be structurally embedded as both individual probes and phased arrays. They can be placed even inside closed cavities during fabrication/overhaul (such as wing structures), and then be left in place for the life of the structure. The embedded

NDE concept opens new horizons for performing in-situ damage detection and structural health monitoring of a multitude of thin-wall structures such as aircraft, missiles, pressure vessels, oil tanks, pipelines, etc.

The paper has presented conclusive experiments that verified that “loud and clear” ultrasonic Lamb waves can be successfully generated with these small, inexpensive, and unobtrusive devices. Wave omnidirectionality and long distance propagation were proven. The pulse-echo crack-detection method was demonstrated on a simple plate specimen and on a realistic aircraft panel.

The arrangement of PWAS in phased arrays has opened additional opportunities, by permitting the sweeping of large areas from a central location. Successful detection of broadside an offside crack in a large plate was illustrated with a simple-to-use graphical user interface (EUSR).

This emerging technology requires a sustained R&D effort to achieve its full developmental potential for applicability to full-scale aerospace vehicles.

ACKNOWLEDGMENT

The collaboration with the Air Force Research Laboratory NDE Branch during the Summer Faculty Fellowship Program 2002 is acknowledged.

References

1. Kropas-Hughes, C.V.; Perez, I.; Winfree, W. P.; Motzer, W. P.; Thompson, R. B. (2002) “Vision of Future Directions of NDE Research” in Review of Quantitative Nondestructive Evaluation Vol. 21, ed. by D. O. Thompson and D. E. Chimenti, American Institute of Physics, Vol. 615, 2002, pp. 2042-2051
2. Rose, J. L. (1995) “Recent Advances in Guided Wave NDE”, 1995 IEEE Ultrasonics Symposium, pp. 761-770
3. Krautkramer (1998) “Emerging Technology – Guided Wave Ultrasonics”, NDTnet, Vol. 3, No. 6, June 1998.
4. Rose, J. L. (2002) “A Baseline and Vision of Ultrasonic Guided Wave Inspection Potential”, ASME Journal of Pressure Vessel Technology – Special Issue on Nondestructive Characterization of Structural Materials, Vol. 124, No. 3, August 2002, pp. 273-282
5. Viktorov, I. A. (1967) Rayleigh and Lamb Waves, Plenum Press, New York, 1967
6. Rose, J. L. (1999) Ultrasonic Waves in Solid Media, Cambridge University Press, 1999
7. Dalton, R. P.; Cawley, P.; Lowe, M. J. S. (2001) “The Potential of Guided Waves for Monitoring Large Areas of Metallic Aircraft Structure”, *Journal of Nondestructive Evaluation*, Vol. 20, pp. 29-46, 2001
8. Thomson, D. O. and Chimenti, D. E. (Editors) (2002) Review of Progress in Quantitative Nondestructive Evaluation, Chapter 2C “Guided Waves” and Chapter 7 “NDE Applications”, AIP Conference Proceedings Vol.

615, 2002

9. Alleyne, D. N.; Cawley P. (1992) “Optimization of Lamb Wave Inspection Techniques”, *NDTE International*, Vol. 25 (1992), No. 1, pp. 11–22
10. Keilers, C. H.; Chang, F.-K. (1995) “Identifying Delamination in Composite Beam using Built-in Piezoelectrics”, *Journal of Intelligent Material Systems and Structures*, Vol. 6, 1995, pp. 647-672
11. Lin, X.; Yuan, F. G. (2001) “Diagnostic Lamb Waves in an Integrated Piezoelectric Sensor/Actuator Plate: Analytical and Experimental Studies”, *Smart Materials and Structures*, Vol. 10, 2001, pp. 907-913
12. Giurgiutiu, V.; Zagrai, A. N.; Bao J.; Redmond, J.; Roach, D.; Rackow, K. (2002) “Active Sensors for Health Monitoring of Aging Aerospace Structures”, *International Journal of the Condition Monitoring and Diagnostic Engineering Management*, UK, Vol. 5, No. 3, August 2002
13. Giurgiutiu, V.; Zagrai, A. (2000) “Characterization of Piezoelectric Wafer Active Sensors”, *Journal of Intelligent Material Systems and Structures*, Technomic Pub., USA, Vol. 11, No. 12, December 2000, pp. 959-976
14. Giurgiutiu, V. (2001) In-situ Structural Health Monitoring, Diagnostics, and Prognostics System Utilizing Thin Piezoelectric Sensors, USC-IPMO Disclosure # 00284, 1/24/2001, U.S. Patent Office Application Serial No. 10-072,644 of February 8, 2002, Attorney Docket No. 16139/09021 (in process)
15. Giurgiutiu, V.; Zagrai, A. N. (2001) “Embedded Self-Sensing Piezoelectric Active Sensors for Online Structural Identification”, *ASME Journal of Vibration and Acoustics*, Vol. 124, January 2001, pp. 116-125
16. Giurgiutiu, V.; Zagrai, A. N.; Bao, J. (2002) “Embedded Active Sensors For In-Situ Structural Health Monitoring of Thin-Wall Structures”, *ASME Journal of Pressure Vessel Technology*, Vol. 124, No. 3, August 2002, pp. 293-302
17. Krautkramer, J.; Krautkramer, H. (1990) *Ultrasonic Testing of Materials*, Springer-Verlag, 1990
18. Lines D.; Dickson K. (1999) “Optimization of High-Frequency Array Technology for Lap-Joint Inspection”, *Proceedings of the 3rd Joint Conference on Aging Aircraft*, 1999, www.galaxyscientific.com/agingaircraft/index2.htm
19. Krautkramer (2002), *Products Catalog*, <http://www.krautkramer.com/arrayweb/default.htm>
20. Giurgiutiu, V.; Bao, J. J. (2002) Embedded-Ultrasonics Structural Radar (EUSR) with Piezoelectric-Wafer Active Sensors (PWAS) for Wide-Area Nondestructive Evaluation of Thin-Wall Structures, USC-IPMO, Disclosure ID No. 00327 of 02/13/2002

Victor Giurgiutiu is an associate professor in the Department of Mechanical Engineering at the University of South Carolina.

For more information contact V. Giurgiutiu, University of South Carolina, Department of Mechanical Engineering, 300 S. Main St., Columbia, SC 29208, email victorg@sc.edu